




Technical Note

# Backscattering Analysis Utilizing Relaxed Hierarchical Equivalent Source Algorithm (RHESA) for Scatterers in Vegetation Medium

Syabeela Syahali <sup>1,\*</sup> , Hong-Tat Ewe <sup>2</sup>, Gobi Vetharatnam <sup>2</sup> and Li-Jun Jiang <sup>3</sup><sup>1</sup> Faculty of Engineering and Technology, Multimedia University, Melaka 75450, Malaysia<sup>2</sup> Lee Kong Chian Faculty Engineering and Science, Universiti Tunku Abdul Rahman, Sg. Long, Kajang 43000, Malaysia<sup>3</sup> Department of Electronic and Electrical Engineering, The University of Hong Kong, Pokfulam, Hong Kong, China

\* Correspondence: syabeela@mmu.edu.my

**Abstract:** The backscattering cross section of cylindrical and elliptical disk-shaped scatterers was investigated in this study, utilising a new numerical solution method called the relaxed hierarchical equivalent source algorithm (RHESA). The results were compared with the backscattering cross section of similar cases, using analytical method validation from literature. The objective of this research was to look into the possibility of replacing analytical methods with the RHESA in volume scattering calculations, and integrating it into modelling the backscattering of layers of dense media for microwave remote sensing in vegetation; as RHESA provides the freedom to model any shape of scatterer, as opposed to the limited shapes available of scatterers in analytical method models. The results demonstrated a good match, indicating that the RHESA may be a good fit for modelling more complicated media, such as vegetation, in future studies.

**Keywords:** microwave remote sensing; relaxed hierarchical equivalent source algorithm (RHESA); volume scattering; vegetation medium



**Citation:** Syahali, S.; Ewe, H.-T.; Vetharatnam, G.; Jiang, L.-J.

Backscattering Analysis Utilizing Relaxed Hierarchical Equivalent Source Algorithm (RHESA) for Scatterers in Vegetation Medium.

*Remote Sens.* **2022**, *14*, 5051. <https://doi.org/10.3390/rs14195051>

Academic Editors: Hongyi Li, Xufeng Wang, Xiaodong Huang, Xiaohua Hao, Xiaoyan Wang and Jian Bi

Received: 27 July 2022

Accepted: 6 October 2022

Published: 10 October 2022

**Publisher's Note:** MDPI stays neutral with regard to jurisdictional claims in published maps and institutional affiliations.



**Copyright:** © 2022 by the authors. Licensee MDPI, Basel, Switzerland. This article is an open access article distributed under the terms and conditions of the Creative Commons Attribution (CC BY) license (<https://creativecommons.org/licenses/by/4.0/>).

## 1. Introduction

Theoretical models in microwave remote sensing research have been developed using analytical methods that employ approximation models [1–12], especially for vegetation media [9–12]. Analytical method models can provide some physical insight into media, and allow the study of scattering behaviour for variations in parameters; however, their accuracy is limited, as this is carried out by approximating the scatterers into limited shapes such as spheres, cylinders, needles, ellipsoids, and elliptic discs. With the development of fast electromagnetic solvers, many large problems can be solved on computers; numerical solution method is rapidly becoming an important mathematical modelling tool for modern electromagnetic engineering [13–15]. In [16–19], a theoretical model for snow media was developed using a new numerical method model—the relaxed hierarchical equivalent source algorithm (RHESA) [20], together with the radiative transfer equation [21]. Using RHESA, snow was modelled in the shapes of spheres, peanuts, droxtals, and hexagonal columns, as opposed to being limited only to spheres in previous approximation models. The scattered values from the scatterers were calculated using RHESA, while the interaction between the scatterers were calculated using the radiative transfer equation. Since the key benefit of using the RHESA would be the ability to represent any shape of scatterer, as opposed to the limited shapes possible in analytic method models, it is interesting to incorporate RHESA into the theoretical modelling of vegetation media, since these media involve scatterers of various complex shapes and sizes. RHESA can be used to calculate the volume scattering of those scatterers, and by using the radiative transfer equation, the complex interactions between scatterers of different orientations in each layer, the

interactions between the layers, and the interactions between the surface and layers, can be calculated accurately compared to analytic methods. In order to achieve that, an important step is to use RHESA in modelling the basic shapes of scatterers in vegetation to compare its backscattering cross section with previous studies that used approximation models. In this study, backscattering analyses for volume scattering for a single cylinder and an elliptic disc-shaped scatterer were performed using RHESA, and compared with the results in [3,5,10,11]. This is carried out to study the prospect of utilising RHESA for volume scattering on a larger scale for vegetation media in the future, as cylinders and elliptic discs are the most common shapes in the vegetation area (representing stems, branches, trunks, and leaves); moreover, their scattering patterns are already available in the literature for comparison and validation purposes.

### 1.1. Analytical Method

In the beginning, Maxwell's equations were solved using closed-form techniques, such as the separation of variables, and special function methods for simple shapes of cylinders, spheres, and ellipsoids. These solutions offer the first physical insight into the nature of electromagnetic field interaction with simple bodies. The generalized Rayleigh–Gans approximation has been used in the study of scattering from circular disks and needles [22], on the basis of very thin oblate spheroids and very narrow prolate spheroids, respectively. For cylindrical scatterers, the infinite cylinder approximation is used [23]. For spherical scatterers, Rayleigh scattering [24,25] is used for sizes that are much smaller than the wavelength, while Mie scattering is used for scatterers with sizes comparable to the wavelength [25]. The scattered field terms for each shape of scatterers were formulated on the basis of these approximations. In [3,5], amplitude and Fresnel phase correction terms were added in the scattered field terms of spheres, circular disks, needles, and cylinders, in order to account for the close distance of the scatterers, and their backscattering cross sections were studied. In [10,11], scattered field terms with Fresnel corrections were derived for general ellipsoids and elliptic disks, based on the generalized Rayleigh–Gans approximation. The backscattering return from the layers of dense media was then modelled using the radiative transfer equation, which was solved iteratively up to the second order to calculate the multiple scattering effect. The coherent effects of a dense medium were considered by the dense medium phase and amplitude correction theory, DMPACT [26].

### 1.2. RHESA

The RHESA can model any 3D object that can be built using 3D modelling software, and overcomes the limitations of analytic method models. This is important in modelling the natural shape of scatterers that are found in real-world plants. The RHESA is a new volume integral equations (VIEs) algorithm that uses the concept of equivalent source in order to link scattered and incident fields. Through the use of an impedance matrix, a relationship between the unknown coefficients and the excitation vector is established, and the equation is solved using the method of moments (MOM) [27,28]. The 3D scatterer is broken into smaller groups in the RHESA. The equivalence surfaces, ES, are then used to enclose them, which become child groups. These child groups are enclosed by the parent groups, forming a hierarchical structure. The equivalent source, to be used to compute the upper level of equivalence source, is the induced current on each ES. The number of unknowns is reduced in this hierarchical form, resulting in faster computation times.

After dividing the scatterer into smaller hierarchical groups using ESs, the RHESA assesses field contributions from the source group,  $G^s$ , to the observer group,  $G^o$ , in three steps: inside-out radiation, translation, and outside-in radiation. In the first step, the  $E$  and  $H$  fields from the primary sources determine the equivalent sources on the spherical ES of group  $G^s$ . In the second stage, these equivalent sources use the Stratton–Chu integral formulation to calculate the radiated  $E$  and  $H$  fields in  $F(G^o)$  from source group  $G^s$ . In the final step, the equivalent sources on the ES of observation group  $G^o$  are determined. The

expression of the radiated electric field  $E^F$  at any position  $r$  inside group  $G^o$  is given by the following:

$$E^F(r) = \sum_{G^s \in F(G^o)} \sum_{f_n \in G^s} I_n C_E^o \left\{ \begin{matrix} \gamma_t^o C_H^s [S_H(f_n)], -\gamma_t^o C_E^s [S_E(f_n)], \\ \gamma_n^o C_E^s [S_E(f_n)] \end{matrix} \right\} \quad (1)$$

where  $S_E$  and  $S_H$  are equivalent sources accounting for electric and magnetic fields;  $C_E$  and  $C_H$  are integral operators from the Stratton–Chu integral formulation representing electric and magnetic fields;  $\gamma_t$  and  $\gamma_n$  are twisted tangential and normal trace operators; and  $f_n$  is the SWG basis function. Details of the formulation can be obtained in [20].

### 2. Methodology

A scatterer’s orientation and geometry are shown in Figure 1. For a cylinder,  $a = b$ , where  $b$  is the cylinder’s radius. The half-length of the cylinder is represented by the value  $c$ . For an elliptic disk,  $a > b$ , and  $c$  becomes very thin. For the backscattering mechanism,  $\theta$  is the incident and scattered angle, and  $d$  is the distance from the scatterer. Scatterers with the same parameters as in the literature [5,10] were chosen for analysis, and their backscattering cross sections were calculated using RHESA, and compared with the backscattering cross sections in [5,10]. The cylinder’s dimensions were set to be  $a = b = 0.2$  cm and  $c = 5$  cm, and the elliptic disk’s dimensions were set to be  $a = 5$  cm,  $b = 2.5$  cm, and  $c = 0.1$  mm. The distance,  $d$  was set at 10 cm for both the scatterers. The relative permittivity was  $9.6-j4.03$  for the cylinder, and  $15-j5$  for the elliptic disk. The background was considered to be free space.

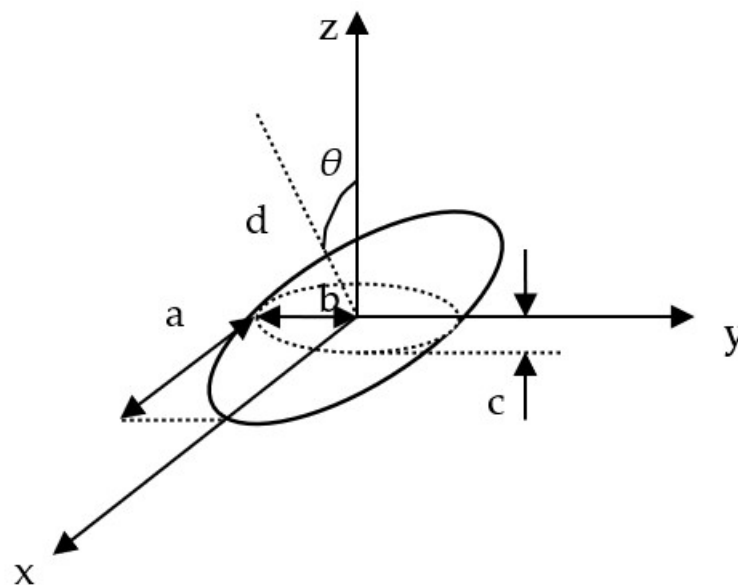


Figure 1. Geometry of a scatterer.

In [3,5,10,11], the backscattering cross section of the scatterer was calculated using the following formula:

$$\sigma = 4\pi |f_{pq}(-\hat{i}, \hat{i})|^2 \quad (2)$$

where  $p$  and  $q$  are the scattered and incident polarization, respectively, and  $f_{pq}$  is the scattering amplitude of the scatterer. The detailed formulation of  $f_{pq}$  with amplitude and Fresnel phase correction term were derived, and are available in [3,5] for cylindrical scatterer, and in [10,11] for elliptical disk scatterer.

In this study, ANSYS software was used to construct and mesh the 3D cylinder and elliptic disk, as shown in Figures 2 and 3, respectively. These meshes were imported to RHESA for processing, as discussed in Section 1.2.

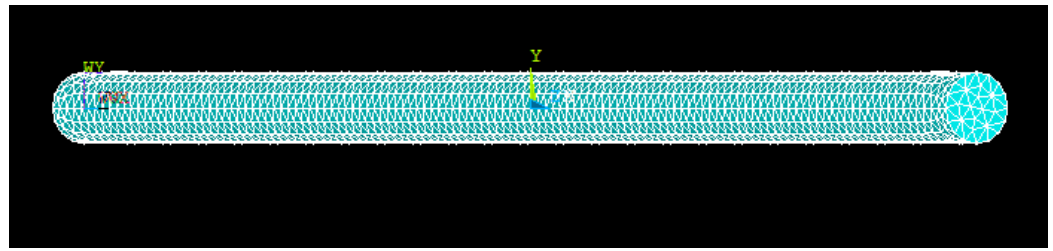


**Figure 2.** 3D cylinder constructed and meshed in ANSYS.

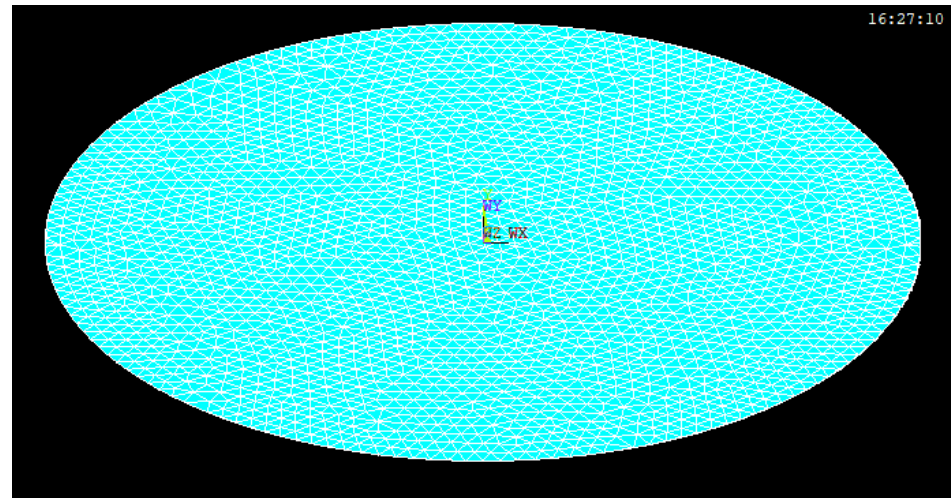


**Figure 3.** 3D elliptic disc constructed and meshed in ANSYS.

RHESA uses the 3D object as input, along with other input parameters such as incident and scattered angles, permittivity, frequency of the wave and coordinates, to calculate the radiated  $E$  and  $H$  fields from a vertically or horizontally polarised incident field. From these radiated fields of RHESA output, the scattered vertical and horizontal fields are derived, and used to model the scattering amplitude,  $f_{pq}$ , in Equation (2) for cylinder and elliptic disc. The backscattering cross section is then calculated using Equation (2), and plotted. The range of study chosen followed [5,10], where the frequency ranged from 0.5 G to 23.9 G, and the incident angle ranged from 20 degrees to 80 degrees. The results were then compared to those in [5] and [10] for validation. For comparison, the results for analytical methods [5,10] were plotted for the backscattering cross section, with and without the amplitude and Fresnel phase correction mentioned in Section 1.1.

### 3. Results

The backscattering cross sections for cylindrical scatterer and elliptical disc scatterer are shown through Figures 4–7 for various values of  $ka$  and incident angles, where  $k$  is the wave number and  $a$  is the scatterer's radius. The results from this study are labelled as the RHESA model; and the results from previous studies, without and with the amplitude and Fresnel phase correction, are plotted and labelled as analytical model (NCT) and analytical model (AFCT), respectively. In Figure 4, the incident angle was fixed at 20 degrees, and backscattering cross section was plotted for  $ka$  from 0.02 to 1 for the cylinder, where the frequency ranged from 0.5 GHz to 23.9 GHz. In Figure 5, the incident angle was fixed at 20 degrees, and backscattering cross section was plotted for  $ka$  from 0.5 to 10 for the elliptic disc, where the frequency ranged from 0.5 GHz to 9.6 GHz. The frequency was then fixed at 9.6 GHz, and backscattering cross sections for both the scatterers were plotted against incident angles of 20 degrees to 80 degrees in Figures 6 and 7. The range of frequency and angle chosen in this study were based on the range studied in [5,10], in order to use the analytical results as a benchmark in investigating the possibility of replacing it with the RHESA.

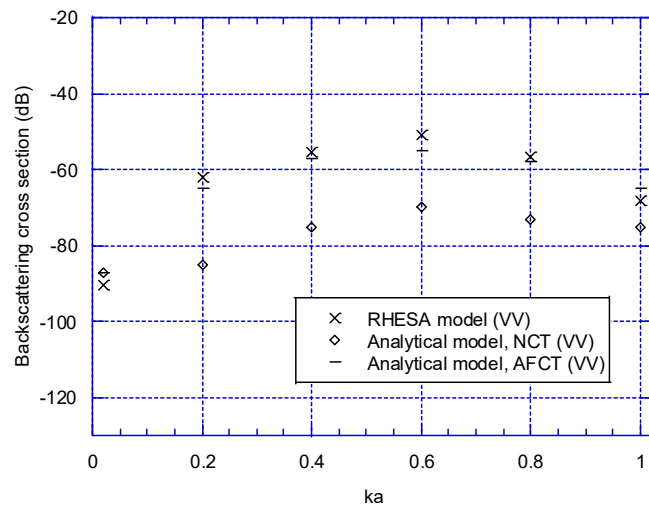


**Figure 4.** Comparison between theories for backscattering cross section of a cylindrical scatterer against  $ka$ , at an incident angle of 20 degrees.

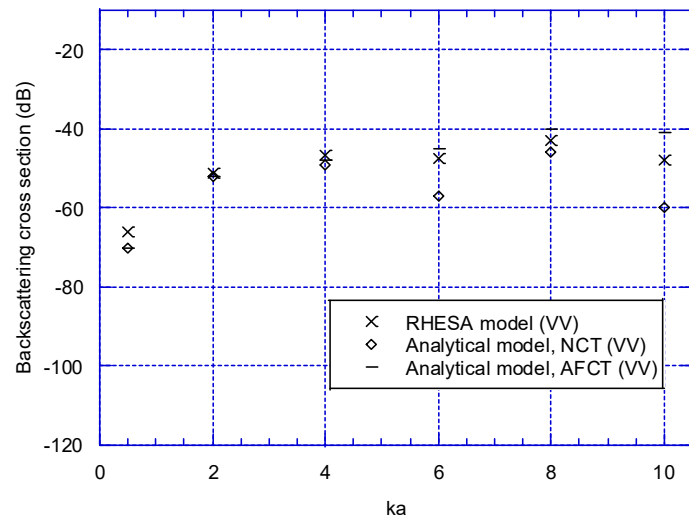


**Figure 5.** Comparison between theories for backscattering cross section of an elliptical disc scatterer against  $ka$ , at an incident angle of 20 degrees.

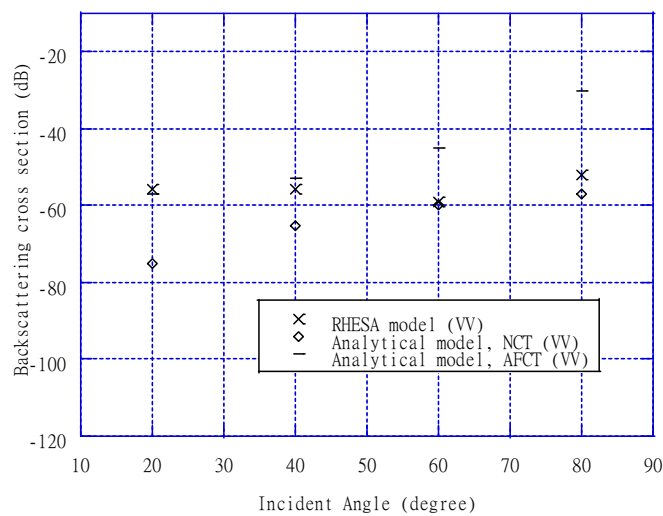


**Figure 6.** Comparison between theories for backscattering cross section of a cylindrical scatterer against incident angle, at a frequency of 9.6 GHz.

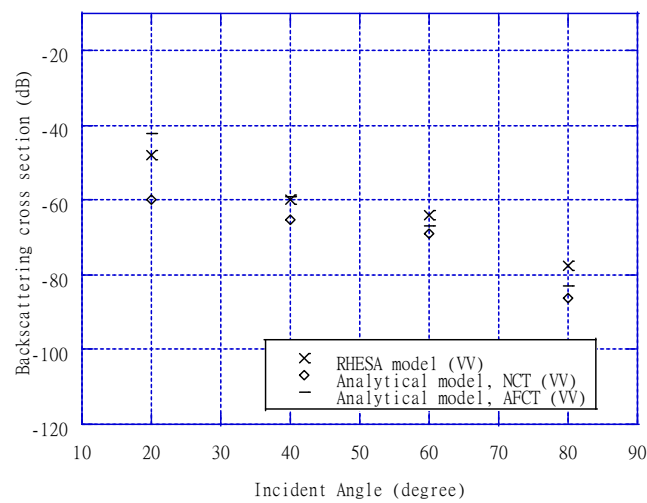


**Figure 7.** Comparison between theories for backscattering cross section of an elliptical disc scatterer against incident angle, at a frequency of 9.6 GHz.

#### 4. Discussion

As can be observed through Figures 4 and 5, the RHESA values are near to the analytical result values with the amplitude and Fresnel phase correction (AFCT), hence showing a promising match in the range of frequencies studied. Results plotted against the incident angles in Figures 6 and 7 also show a good match with the analytical result values with the amplitude and Fresnel phase correction (AFCT); the exception occurred at higher incident angles in Figure 6, where the backscattering cross section for the cylinder from RHESA approached those of the analytical results, without the amplitude and Fresnel correction (NCT).

In order to further analyse the pattern observed in Figure 6 at higher incident angles, analytical results of backscattering cross section with only the Fresnel phase correction [3,5,10], were added into the graphs for the entire range studied in this paper. This is carried out to analyse the effect of the Fresnel phase correction and the effect of the amplitude correction separately for the region studied. It was found that the Fresnel phase correction was very dominant and important in the region of higher incident angles in Figure 6, compared to other region in this study. Figure 8 shows the results from Figure 6 after adding the analytical results with Fresnel phase correction, labelled as Analytical model (FCT).

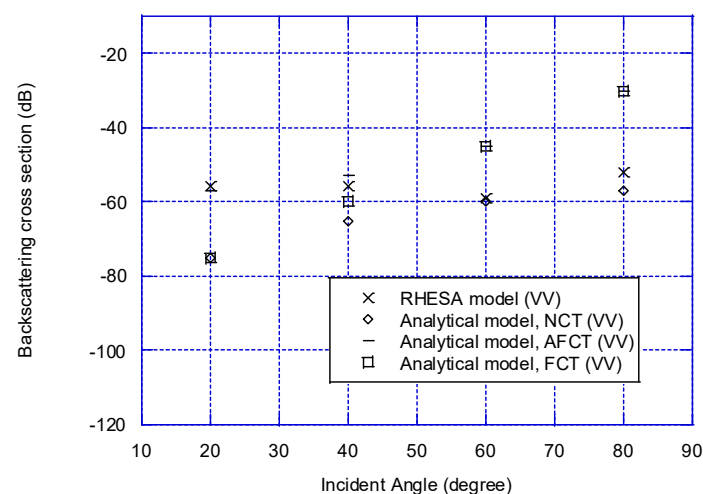


**Figure 8.** Comparison between theories for backscattering cross section of a cylindrical scatterer against incident angle, at 9.6 GHz frequency, with added results from analytical models with Fresnel phase corrections.

The pattern shown in Figure 8 is in line with the findings in [3,5], where the Fresnel phase correction becomes important when the incident angle approaches 90 degrees, and when the scattering comes from the larger dimension of the scatterer; some scatterers have one dimension that is much smaller than the other dimension, such as needles and cylinders. This suggests that the RHESA may not be accurate in this condition.

However, the results from analytical method and RHESA comparisons generally show a promising match in this study, hence demonstrating that the RHESA can be used to calculate volume scattering instead of the analytical model, especially at lower incident angles. In future, this study can be extended to a layer or to layers of scatterers, as in real vegetation media, with the ability to model more realistic shapes of scatterers. By combining the RHESA with radiative transfer theory solution and DMPACT, the total backscattering return from layers of dense media can be modelled as in previous studies [2,5,7,8,11], but with more accurate results for vegetation media.

## 5. Conclusions

In this study, a theoretical scattering model was proposed by utilising the RHESA to model scatterers. Backscattering cross section was calculated for a cylinder and an elliptical disk; when compared with other theories, RHESA appears to have a good prospect of being used in microwave remote sensing on vegetation media in the future.

**Author Contributions:** Conceptualization, methodology, formal analysis, writing—original draft preparation, S.S.: writing—review and editing, supervision, H.-T.E. and G.V.; funding acquisition, project administration, resources, S.S., H.-T.E., G.V. and L.-J.J. All authors have read and agreed to the published version of the manuscript.

**Funding:** This project was funded by [Multimedia University IRFund] grant number [MMUI/210017] and [Asian Office of Aerospace R&D (AOARD)] grant number [FA2386-12-14082].

**Conflicts of Interest:** The authors declare no conflict of interest.

## References

- Ishimaru, A. *Wave Propagation and Scattering in Random Media*; Academic Press: New York, NY, USA, 1978; Volume 2.
- Ewe, H.T.; Chuah, H.T.; Fung, A.K. A backscatter model for a dense discrete medium: Analysis and numerical results. *Remote Sens. Environ.* **1998**, *65*, 195–203. [[CrossRef](#)]
- Ewe, H.T.; Chuah, H.T. A study of Fresnel scattered field for non-spherical discrete scatterers. *Prog. Electromagn. Res.* **2000**, *25*, 189–222. [[CrossRef](#)]
- Ao, C.O. *Electromagnetic Wave Scattering by Discrete Random Media with Remote Sensing Applications*. Ph.D. Thesis, University of California, Berkeley, CA, USA, 2001.
- Ewe, H.T. *A Microwave Scattering Model for an Electrically Dense Discrete Random Medium*. Ph.D. Thesis, Multimedia University, Cyberjaya, Malaysia, 1999. Unpublished doctoral dissertation.
- Wu, T.D.; Chen, K.S.; Shi, J.; Lee, H.W.; Fung, A.K. A study of an AIEM model for bistatic scattering from randomly rough surfaces. *IEEE Trans. Geosci. Remote Sens.* **2008**, *46*, 2584–2598.
- Syahali, S.; Ewe, H.T. Backscattering Analysis for Snow Remote Sensing Model with Higher Order of Surface-Volume Scattering. *Prog. Electromagn. Res. M* **2016**, *48*, 25–36. [[CrossRef](#)]
- Syahali, S.; Ewe, H.T. Remote Sensing Backscattering Model for sea ice: Theoretical modelling and Analysis. *Adv. Polar Sci.* **2013**, *24*, 248–257.
- Eom, H.J.; Fung, A.K. A scatter model for vegetation up to Ku-band. *Remote Sens. Environ.* **1984**, *15*, 185–200. [[CrossRef](#)]
- Koay, J.Y.; Ewe, H.T.; Chuah, H.T. A Study of Fresnel Scattered Fields for Ellipsoidal and Elliptic-Disk-Shaped Scatterers. *IEEE Trans. Geosci. Remote Sens.* **2008**, *46*, 1091–1103. [[CrossRef](#)]
- Koay, J.Y.; Lee, Y.J.; Ewe, H.T. and Chuah, H.T. *Electromagnetic Wave Scattering in Dense Media: Applications in the Remote Sensing of Sea Ice and Vegetation*. In *Electromagnetic Scattering: A Remote Sensing Perspective*; WSPC: Singapore, 2017; pp. 303–339.
- Toh, C.M.; Ewe, H.T.; Tey, S.H.; Tay, Y.H. A Study on Oil Palm Remote Sensing at L-Band with Dense Medium Microwave Backscattering Model. *IEEE Trans. Geosci. Remote Sens.* **2019**, *57*, 8037–8047. [[CrossRef](#)]
- Li, M.; Chew, W.C. Wave-Field Interaction with Complex Structures. *IEEE Trans. Antennas Propag.* **2007**, *55*, 130–138. [[CrossRef](#)]
- Velamparambil, S.; Chew, W.C.; Song, J. 10 Million Unknowns: Is It That Big? *IEEE Antennas Propagation Mag.* **2003**, *45*, 43–58. [[CrossRef](#)]
- Sumithra, P.; Thiripurasundari, D. Review on Computational Electromagnetics. *Adv. Electromagn.* **2017**, *6*, 42. [[CrossRef](#)]

16. Lum, C.F.; Fu, X.; Ewe, H.T.; Jiang, L.J. A study of scattering from snow embedded with non-spherical shapes of scatterers with Relaxed Hierarchical Equivalent Source Algorithm (RHESA). *Prog. Electromagn. Res. M* **2017**, *61*, 51–60. [[CrossRef](#)]
17. Lum, C.F.; Ewe, H.T.; Xin, F.; Jiang, L.J.; Chuah, H.T. An analysis of scattering from snow with relaxed hierarchical equivalent source algorithm. In Proceedings of the 2017 IEEE International Geoscience and Remote Sensing Symposium (IGARSS), Fort Worth, TX, USA, 23–28 July 2017; IEEE: Piscataway, NJ, USA, 2017; pp. 1434–1437.
18. Lum, C.F.; Fu, X.; Ewe, H.T.; Jiang, L.J. A Study of Scattering from a Layer of Random Discrete Medium with Hierarchical Equivalent Source Algorithm (HESA). In Proceedings of the Progress in Electromagnetic Research Symposium (PIERS), Shanghai, China, 8–11 August 2016.
19. Kumaresan, H.A.; Ewe, H.T.; Vetharatnam, G.; Jiang, L.-J. Model Computation with Second-Order Radiative Transfer Equation for Snow Medium Using Coupled Finite Element Method and Method of Moment and Relaxed Hierarchical Equivalent Source Algorithm. In Proceedings of the 2021 IEEE International Geoscience and Remote Sensing Symposium IGARSS, Brussels, Belgium, 11–16 July 2021; pp. 1417–1420.
20. Fu, X.; Jiang, L.J.; Ewe, H.T. A novel relaxed hierarchical equivalent source algorithm (RHESA) for electromagnetic scattering analysis of dielectric objects. *J. Electromagn. Waves Appl.* **2016**, *30*, 1631–1642. [[CrossRef](#)]
21. Chandrasekhar, S. *Radiative Transfer*; Dover: New York, NY, USA, 1960.
22. Karam, M.A.; Fung, A.K. Leaf-shape effects in electromagnetic wave scattering from vegetation. *IEEE Trans. Geosci. Remote Sens.* **1989**, *27*, 687–697. [[CrossRef](#)]
23. Fung, A.K. *Microwave Scattering and Emission Models and Their Applications*; Artech House: Norwood, MA, USA, 1994.
24. Stratton, J.A. *Electromagnetic Theory*; McGraw-Hill: New York, NY, USA, 1941.
25. Van de Hulst, H.C. *Light Scattering by Small Particles*; John Wiley and Sons: New York, NY, USA, 1957.
26. Chuah, H.T.; Tjuatja, S.; Fung, A.K.; Bredow, J.W. A phase matrix for a dense discrete random medium: Evaluation of volume scattering coefficient. *IEEE Trans. Geosci. Remote Sens.* **1996**, *34*, 1137–1143. [[CrossRef](#)]
27. Gibson, W.C. *The Method of Moments in Electromagnetics*; Taylor & Francis Group, LLC: Oxfordshire, UK, 2008.
28. Jin, J.; Chew, W.C. *Computational Electromagnetics: The Method of Moments*; The Electrical Engineering Handbook; Elsevier Inc.: Amsterdam, The Netherlands, 2005.